Optics Communications 283 (2010) 3564–3568

Contents lists available at ScienceDirect

Optics Communications

journal homepage: www.elsevier.com/locate/optcom

Symmetry property of a generalized Billet's *N*-split lens

Chieh-Jen Cheng, Jyh-Long Chern *

Department of Photonics, Institute of Electro-Optical Engineering, National Chiao Tung University, Hsinchu 300, Taiwan, ROC

ARTICLE INFO

Article history:
Received 17 March 2010
Received in revised form 11 May 2010
Accepted 11 May 2010

Keywords:
Diffraction
Paraxial wave optics
Billet's split lens

ABSTRACT

This study examines the diffraction properties of a generalized split *N*-sector lens originating from Billet's split bi-sector lens. The intensity distributions vary dramatically as the number of split sectors increases, and especially compared with those of the classical Billet's split lens. Nevertheless, the type of lens splitting selected causes the interference pattern of equidistant straight lines in the original Billet's lens to form an *N*-fold angularly distributed pattern with an angle difference of $2\pi/N$. For an odd number of splitting *N*, there is an additional angle shift of π/N for the azimuthally distributed patterns of equidistant straight lines. In other words, there are two kinds of symmetry even for simple splitting operations. On the other hand, the peak intensity distribution in the central portion resembles a concentric-circle-like pattern, when *N* is large as a result of *N*-beam interference.

1. Introduction

The study of field propagation and its associated diffraction behavior is a classical topic in optics research [1]. Previous studies show that this topic has many important applications in optical testing [2] and the development of new optical devices using nano-technology [3]. The current design approach for creating optical products is still primarily based on ray optics, while diffraction-based theory generally provides a reference and base line of resolution and performance limitations. Nevertheless, the diffraction theory of optical fields remains an important research topic. Researchers continue to make active progress in this area, as indicated by the selected works of E. Wolf [4]. In viewing the demands of technology development and academic interest, some of our early attentions were dedicated to exploring far-field behavior with sub-wavelength variations, where aperture (stop) plays a key role in information retrieval [5]. In existing literature, the aperture stop (circular and rectangular) and perfect lens are classical platforms for exploring diffraction behavior. Studies on this topic generally fall into one of two categories:

(1) Light sources could be different, e.g., a cylindrical beam or a vector polarized beam.
(2) The lens can have aberrations, defocus, or coma.

The current study considers a different approach that may be able to provide an additional basic reference for diffraction study, namely the generalized form of a split lens.

There are many ways to achieve lens splitting; for example, in a configuration of Meslin's experiment or using Billet's split lens [6]. Once a lens is split in multiple pieces, the resulting interference involves multiple beams and the configuration of multiple paths. This creates complicated beam propagation and interference. Nevertheless, if this generalization is implemented symmetrically, the field distribution exhibits an embedded symmetry, which reduces and simplifies the complexity of analysis and calculation. Thus, exploring the diffraction behavior with such a generalization, particularly the symmetry properties, is worthy of further research. Therefore, this study presents such a generalization of Billet's split lens. Note that previous research has developed such a Billet's split lens for multiple imaging and multichannel optical processing [7].

This paper is organized as follows. Section 2 briefly describes the diffraction theory and analytically deduces the symmetry properties with respect to optical axis. Section 3 numerically explores the interference pattern, with a focus on the far-field symmetry properties during lens splitting. Finally, Section 4 provides conclusions.

2. Theoretical exploration

The bottom of Fig. 1 shows a schematic diagram of Billet's split bi-sector lens, where a conventional focusing lens is split into two identical halves (two sectors). The upper half and the lower half are then moved a distance *d* up and down the *Y*-axis, respectively. This split lens creates a collimated uniform monochromatic wave with a wavelength of λ for two different foci, F_1 and F_2, in the focal plane. The diffraction theory applied here assumes that the aperture radius $a \gg \lambda$, the focal length $f \gg a \gg \lambda$, and the Fresnel number $a^2/\lambda f$ is much larger than unity. When the (half) translation length *d* is zero, the two foci will coincide and the integral representation of the disturbance $U(P)$ at a point $P(x,y,z)$ in the image space is [6]

$$U(P) = -\frac{i}{\lambda}\frac{a^2 A}{f^2} e^{i\left(\frac{f}{a}\right)^2 u} \int_0^1 \int_0^{2\pi} e^{-i\left[v\rho\cos(\theta-\psi) + \frac{1}{2}u\rho^2\right]} \rho d\rho d\theta, \quad (1)$$

* Corresponding author. Tel.: +886 3 5712121x56348.
E-mail addresses: cjcheng.eo92g@nctu.edu.tw (C.-J. Cheng), jlchern@faculty.nctu.edu.tw (J.-L. Chern).

0030-4018/$ – see front matter © 2010 Elsevier B.V. All rights reserved.
doi:10.1016/j.optcom.2010.05.024

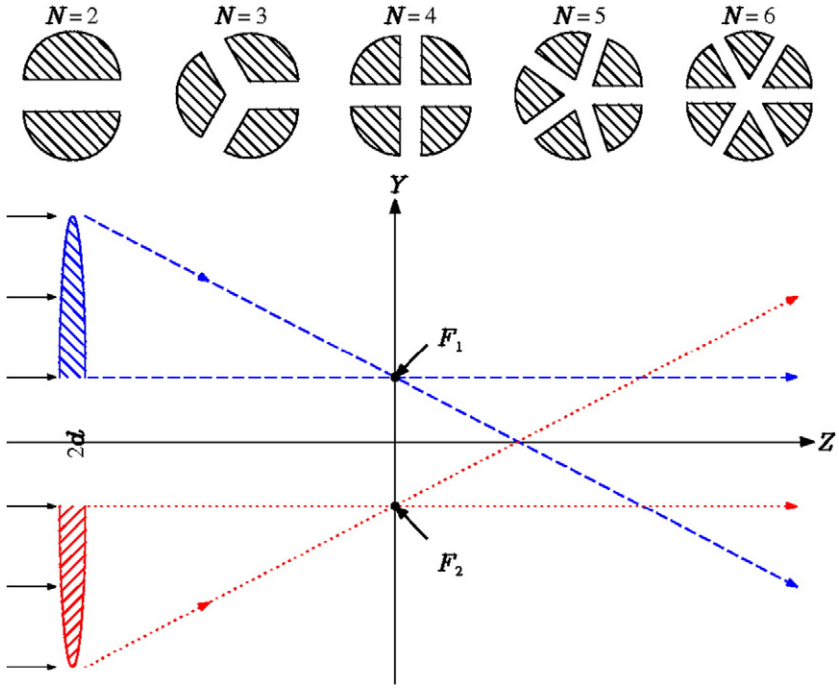

Fig. 1. *Top*: Front view from the left side, showing the arrangements of sectors when $N=2$, 3, 4, 5, and 6, where N is the number of sectors. *Bottom*: Schematic diagram of Billet split bi-sector lens. F_1 and F_2 are the first focus and second focus, respectively, and $2d$ is the separation distance between the foci of the two sectors.

where the optical units u, v, and ψ represent the Cartesian coordinate positions of P (x, y, z). These values are $u = \frac{2\pi}{\lambda}\left(\frac{a}{f}\right)^2 z$, $v = \frac{2\pi}{\lambda}\left(\frac{a}{f}\right) r = \frac{2\pi}{\lambda}\left(\frac{a}{f}\right)\sqrt{x^2+y^2}$, where $x = r\cos\psi$ and $y = r\sin\psi$. Fig. 2 shows the coordinate system. The disturbance $U(P)$ is

$$U(P) = C\int_0^1 e^{-i\frac{1}{2}u\rho^2}\int_0^{2\pi} e^{-i\left[\frac{2\pi}{\lambda}\frac{a}{f}\rho[x\cos\theta + y\sin\theta]\right]} d\theta\rho d\rho, \tag{2}$$

where $C = -\frac{i}{\lambda}\frac{a^2 A}{f^2} e^{i\left(\frac{f}{a}\right)^2 u}$.

To generalize lens splitting, a focusing lens is divided into N equiangular sectors. Each sector is exploded and translated a distance d in the r direction along the perpendicular bisector of the angle. Fig. 1 shows the schematic layouts of the simplest cases of $N=2$, 3, 4, 5, and 6. Ray-based analysis shows that the foci of all sectors constitute a regular N-sided polygon in the focal plane. Therefore, the focal point of each sector is

$$\begin{aligned} x_m &= d\cos\psi_m, \\ y_m &= d\sin\psi_m, \\ \psi_m &= \frac{2\pi}{N}(m+1/2), \quad m = 0, 1, .., N-1. \end{aligned} \tag{3}$$

By applying coordinate translation and summing the contributions from all sectors, the disturbance $U(P)$ is

$$U(P) = C\int_0^1 e^{-i\frac{1}{2}u\rho^2}\sum_{m=0}^{N-1}\int_{m\frac{2\pi}{N}}^{(m+1)\frac{2\pi}{N}} e^{-i\left[\frac{2\pi}{\lambda}\frac{a}{f}\rho[(x-x_m)\cos\theta + (y-y_m)\sin\theta]\right]} d\theta\rho d\rho, \tag{4}$$

Substituting Eq. (3) into Eq. (4) leads to

$$U(P) = C\int_0^1 e^{-i\frac{1}{2}u\rho^2}\sum_{m=0}^{n-1}\int_{m\frac{2\pi}{N}}^{(m+1)\frac{2\pi}{N}} e^{-i\left\{\frac{2\pi}{\lambda}\frac{a}{f}\rho[r\cos(\theta-\psi)-d\cos(\theta-\psi_m)]\right\}} d\theta\rho d\rho \tag{5}$$

After changing the interval of integration for each segment to the same value, the d term in the brackets of exponential function is no longer a function of m. The summation can be put into the integrand of r term only, i.e.,

$$U(P) = C\int_0^1 e^{-i\frac{1}{2}u\rho^2}\int_0^{\frac{2\pi}{N}} e^{iv_d\rho\cos\left(\theta-\frac{\pi}{N}\right)} \times \sum_{m=0}^{N-1} e^{-iv\rho\cos\left(\theta-\psi+m\frac{2\pi}{N}\right)} d\theta\rho d\rho, \tag{6}$$

where $v_d = \frac{2\pi}{\lambda}\left(\frac{a}{f}\right)d$. Now, the azimuthally symmetrical property at a specific z plane with respect to the optical axis is

$$U(u, v, \psi - \frac{2\pi}{N}) = U(u, v, \psi), \tag{7}$$

This shows that a disturbance on a specified z plane is rotationally symmetrical with an angle of $2\pi/N$. In other words, the disturbance repeats itself every $2\pi/N$ along the azimuthal direction, and hence, an N-fold rotational symmetry originates from the symmetry in the split form in the lens.

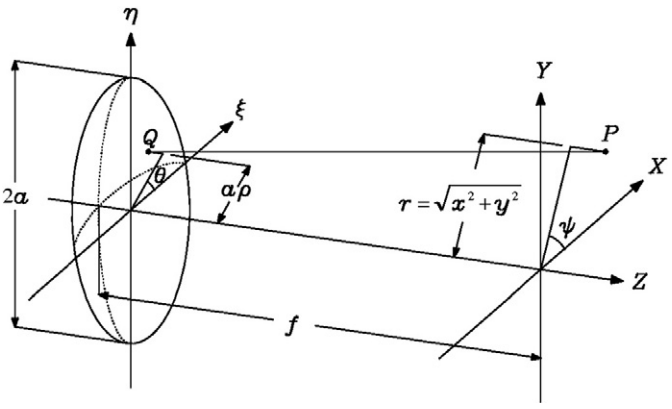

Fig. 2. Notation representation of the coordinate system of beam propagation.

3. Numerical exploration

This section explores the light distribution using numerical simulations. To fulfill the condition of diffraction beam, i.e., the numerical aperture should be around 0.1, we used a typical lens with a focal length of a few ten mm, e.g., $f=30{,}000\lambda$, to create an aperture radius $a=3000\lambda$. This lens also has the (half) separation distance $d=100\lambda$. For the numerical example of $\lambda=630$ nm, these settings lead to $f=18.9$ mm, $a=1.89$ mm, and $d=0.063$ mm. The plot of intensity distributions was normalized to 100. As a base reference, we revisited the classical Billet spilt lens, i.e., $N=2$. After the focal plane, the interference pattern in the *XY*-plane formed within the overlap region lit by two sectors. The intensity distribution in Fig. 3(a) reflects this result, clearly showing a two-fold symmetry [6]. The diffraction pattern contributed from each sector beyond the focal plane is similar to the original half sector, but rotated π radians around the new translated axis. This new translated axis is parallel to the optical axis throughout the focus of each sector. The lights from the two semicircles form a overlapped region near the optical axis and create interference. The interference patterns, therefore, are equidistant straight lines parallel to the lines that cut the spherical wavefront into two hemispheres, and are perpendicular to the line through two focal points F_1 and F_2. On the other hand, the diffraction patterns outside the overlapped region lit by two sectors are hyperbolas, which are sections of hyperboloids of revolution about the F_1F_2 axis and have F_1 and F_2 as common foci [6].

To identify how splitting a lens changes the intensity distribution, this study evaluates the distributions for $N=2$ to $N=10$ in the far field (here, $z=5000\lambda=3.15$ mm, if $\lambda=630$ nm). Fig. 3(b) shows that a 3-fold symmetry is readily apparent when $N=3$. However, the fringes of hyperbolas must have near $2\pi/3$ radians, instead of π radians in the case of $N=2$. In the case of $N=2$, they are in the opposite direction of the equidistant straight lines, and the fringes of equidistant straight lines in the *XY*-plane appear inside the overlap region lit by each two sectors. On the other hand, for the case of $N=3$, there are three distinct straight-line fringes that are parallel to three lines located at the angles of $\pi/3$, π, and $5\pi/3$, respectively. Nevertheless, these three lines do not coincide with the lines of sector division, but rotate an additional angle of $\pi/3$ around the optical axis. This is because the diffraction pattern of each sector (beyond the focal plane) rotates π radians around each translated axis parallel to optical axis through the focus of each sector. In addition, the two straight cutting edges of each sector also rotate by π radians, and therefore interfere with each other after a rotation of the azimuthal angle of π. When N is odd, the rotation prevents the interference pattern of each straight line from coinciding with the original cutting edge of each sector, and all fringes of straight lines resemble an angle of rotation of π/N-radian (mod 2π) around the optical axis. When N is even, the rotation of the azimuthal angle of π also shifts the interference pattern of straight line π radians, but the rotated interference pattern of straight lines coincides with the original cutting edge of other sectors due to reflection symmetry between the *X*- and *Y*-axes. Under these circumstances, all straight line fringes look like they have not rotated, and remain located within the cutting edge of each sector. Similarly, the interference pattern of equidistant straight lines by an *N*-split lens is oriented at the angle of $m\cdot 2\pi/N$ when N is an even number For the case of odd-number lens splitting, the interference pattern is at the angle of $\pi/N+m\cdot 2\pi/N$, which requires an additional angle shift of π/N.

Next, consider the central region of intensity distribution near the optical axis. Fig. 3 indicates that as N becomes larger, the intensity distribution centered on a specified location along the optical axis begins to resemble a concentric-circle-like interference pattern, while for a small

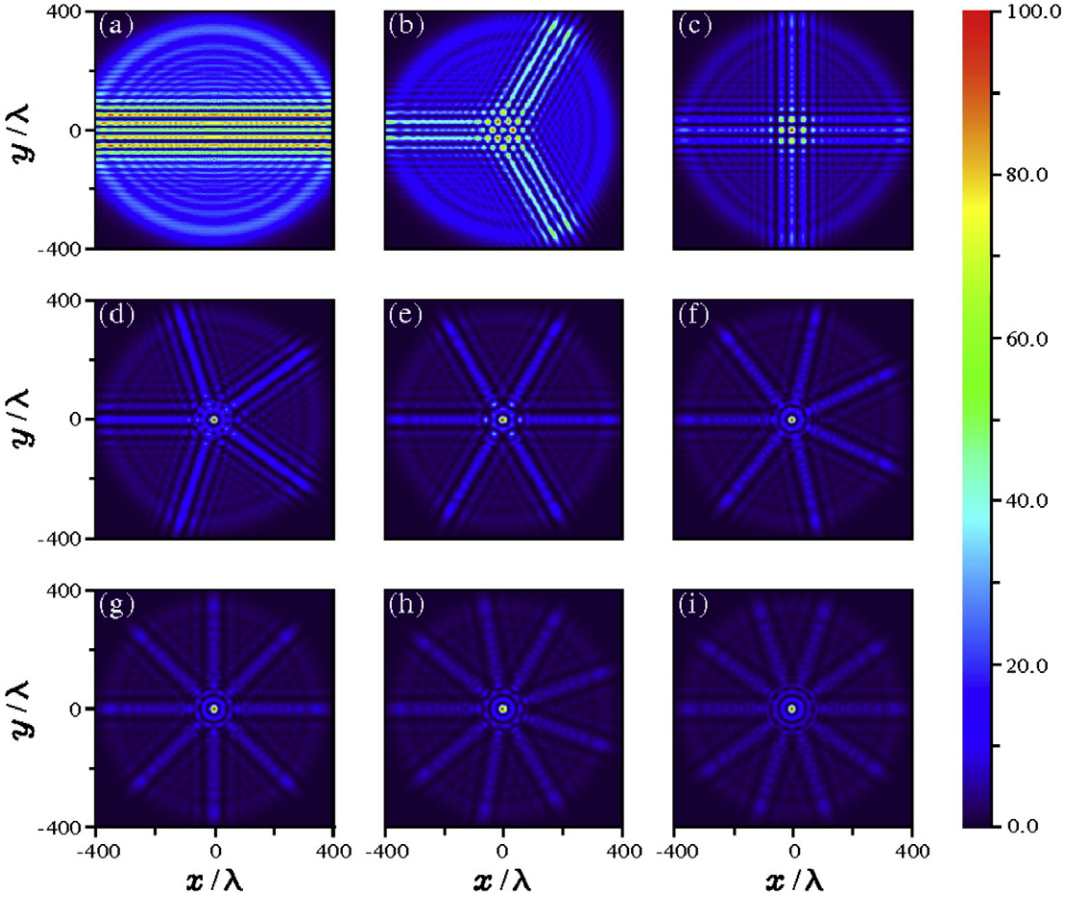

Fig. 3. Density plot of normalized intensity distribution of the generalized *N*-split lens in the *XY*-plane at $z=5000\lambda$ where (a) $N=2$, (b) $N=3$, (c) $N=4$, (d) $N=5$, (e) $N=6$, (f) $N=7$, (g) $N=8$, (h) $N=9$, and (i) $N=10$.

N, the distribution is more like a regular N-sided polygon. This polygon basically represents the split distance d, i.e., the circumradius is limited by d. The intensity distribution in the central region involves multiple-beam interference, i.e., all sectors contribute to the total field. However, only the beam interference of two sectors, i.e., the overlap of the field from two sectors causes the straight-line-like interference pattern in the outward azimuthal regime. For example, consider the case of $N=12$, where Fig. 4(b) plots the far-field intensity distribution ($z=5000\lambda$ for simplification). The central regime contains concentric-circle-like interference patterns. The second bright ring actually has twelve peaks, and each of which is located along the azimuthal direction with an angle difference of $\pi/6$. However, the difference between the minimum and maximum intensity of the second bright ring is too small to identify in Fig. 4(b). Therefore, Fig. 4(c) presents an enlargement of Fig. 4(b). Here, the peak distributions are readily apparent in the inner rings, and twelve peaks clearly appear in the second and fourth bright rings. From the symmetrical properties deduced above, numerical simulation reveal that the distance between two successive peaks is $\sim d\cos(\pi/12)\sim 0.122$ mm, if $\lambda=630$ nm, where the peak location is defined according to the maximum, even at such a far-field distance. Numerical simulations also show that as N becomes larger, the concentric-circle-like interference patterns inside the region of circumscribed circle become significant at various XY-planes, i.e., at *any* specified locations along the optical axis, provided that the interference occurs after the focal plane. However, the symmetry properties deduced above remain the same.

4. Conclusions

In conclusion, the diffraction behavior of a generalized Billet's N-split lens has been derived based on symmetry consideration. The intensity distributions vary significantly as the number of split sectors increases, particularly compared with the original Billet's split lens. Nevertheless, there is a symmetry relationship embedded in this class of split lenses. Due to lens-splitting form adopted in this study, the intensity distribution has an N-fold rotational symmetry with respect to the optical axis in the XY-plane. The interference patterns of equidistant straight lines are orientated at the angle of $m\cdot 2\pi/N$ when N is even, but at the angle of $\pi/N+m\cdot 2\pi/N$ when N is odd, where $m=0, 1, 2,\ldots, N-1$. In other words, there are two kinds of symmetry even though the corresponding splitting operation is simple. The interference of the disturbance by two adjacent sectors of the split lens is the physical origin of the fringes of equidistant straight lines. In addition, this symmetrical property is physically traceable based on the symmetry embedded in the splitting form of lens.

A concentric-circle-like interference pattern near the optical axis appears when N is larger than 10. This feature is primarily due to multiple-beam interference. The multiple-beam interference inside the inner regime forms a polygon boundary of intensity distribution in which the distance between two successive maximum peaks is $\sim d\cos(\pi/N)$. When the number of sectors in split lens becomes very large, the polygon nearly becomes a circle.

Note that the symmetry embedded within the generalized split lens and the straight-line provide two basic guidelines for forming the azimuthal light distribution while the central regime hosts a concentric-like distribution. Practically, the proposed approach to the generalized split lens provides more means of controlling light beams. Though this study is limited to Billet's split lens, different symmetrical forms in lens splitting will lead to different kinds of light distribution. It is also possible to implement this generalized Billet's N-split lens with liquid crystal, i.e., a segmented-aperture optical system in which phase-shifting material, here liquid crystal, fills each segmented region [8,9].

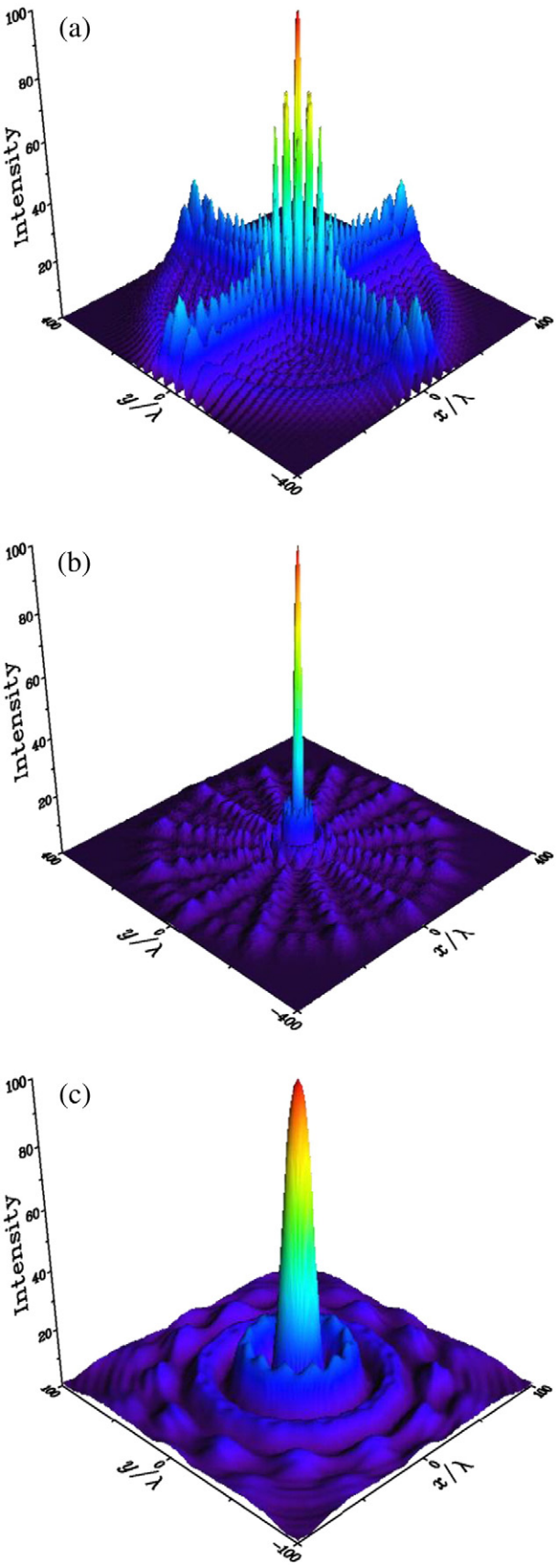

Fig. 4. Normalized intensity distribution of the generalized N-split lens in the XY-plane at $z=5000\lambda$ where (a) $N=4$, (b) $N=12$, and (c) Enlargement of (b).

Acknowledgements

We thank the anonymous reviewer for the suggestion of phase-shifting material as one possible implementation. This work is

partially supported by the National Science Council, Taiwan, ROC, under project NSC-96-2628-E-009-019-MY3.

References

[1] M. Mansuripur, Classical Optics and its Applications, 2nd. EdCambridge University Press, 2009.
[2] D. Malacara, Optical Shop Testing, 3rd. EdWiley Interscience, 2007.
[3] L. Novotny, B. Hecht, Principles of Nano-Optics, Cambridge University Press, 2006.
[4] E. Wolf, Selected Works of E. Wolf, with Commentary, World Scientific, 2001.
[5] S.-C. Chu, J.-L. Chern, Opt. Lett. 29 (2004) 1045;
J. Opt. Soc. Am. A 23 (2006) 2471;
Opt. Commun. 281 (2008) 1997.
[6] M. Born, E. Wolf, Principles of Optics, 7th expended ed, Cambridge University Press, 1999.
[7] A. Senthil Kumar, R.M. Vasu, Appl. Opt. 26 (1987) 5345.
[8] D. Dayton, S. Sandven, J. Gonglewski, S. Browne, S. Rogers, S. Mcdermott, Opt. Express 1 (1997) 338.
[9] E.J. Fernández, P.M. Prieto, P. Artal, Opt. Express 17 (2009) 11013.